Journal of Alloys and Compounds 509 (2011) 7498–7503

Contents lists available at ScienceDirect

Journal of Alloys and Compounds

journal homepage: www.elsevier.com/locate/jallcom

# Lattice defects introduced into $LaNi_5$-based alloys during hydrogen absorption/desorption cycling

Junko Matsuda*, Yumiko Nakamura, Etsuo Akiba

*Energy Technology Research Institute (ETRI), National Institute of Advanced Industrial Science and Technology (AIST), Tsukuba, Ibaraki 305-8565, Japan*

ARTICLE INFO

*Article history:*
Received 6 December 2010
Accepted 17 April 2011
Available online 23 April 2011

*Keywords:*
$LaNi_5$-based alloys
Hydrogen absorption
Misfit dislocation
Transmission electron microscopy

ABSTRACT

$LaNi_5$-based intermetallic compounds before and after hydrogen absorption/desorption cycling were observed by transmission electron microscopy. Both a-type and c-type dislocations, which had respective Burgers vectors of $1/3 < 11\bar{2}0 >$ and <0001> in the $\{01\bar{1}0\}$ slip plane, were introduced into $LaNi_5$, $LaNi_{4.5}Cu_{0.5}$ and $LaNi_{4.5}Fe_{0.5}$ after the first absorption/desorption cycle. These alloys exhibited large difference in the equilibrium pressure between the first absorption and first desorption. Dislocations were introduced during hydrogenation in order to accommodate lattice mismatch between the metal-hydrogen solid solution and the metal hydride; furthermore, the interface between the solid solution and hydride was suggested to be the $\{01\bar{1}0\}$ plane. In contrast, neither dislocations nor stacking faults were observed in $LaNi_{4.5}Si_{0.5}$, $LaNi_{4.5}Al_{0.5}$ and $LaNi_{4.75}Sn_{0.75}$, which showed little or no hysteresis in the hydrogen pressure–composition isotherms. Excess pressure was needed in the absorption process for the formation of misfit dislocations.



## 1. Introduction

Since Van Vucht et al. have reported that the $LaNi_5$ rapidly absorbs more than six atoms of hydrogen atoms per formula unit under a hydrogen pressure of about 0.25 MPa at room temperature [1], many researchers have investigated $LaNi_5$-based compounds with the aim of using them in practical applications such as Ni-MH batteries. The preparation of pseudobinary compounds by partial replacement of the constituents of $LaNi_5$ has been investigated as a means of lowering production costs and improving hydriding properties, especially reversibility. In fact, almost all La sites are occupied by rare-earth elements, while the Ni sites can be partially substituted with 3d transition metals having different levels of solid solubility [2–4].

$LaNi_5$ and related alloys have been reported to show significant anisotropic line broadening in X-ray diffraction patterns [5]. It is also known that the equilibrium pressure of the first hydrogenation of $LaNi_5$-based alloys, including binary $LaNi_5$, is higher than that after the second hydrogenation [4]. However, not all $LaNi_5$-based alloys exhibit such behavior [5,6]. It has been reported that these two phenomena are related to each other [7] and that they are strongly associated with cycling lifetime and other practical properties [4,8].

In situ X-ray measurements using a high-pressure hydrogen cell have revealed that anisotropic line broadening of hk0 occurs in only the hydride phase of $LaNi_5$ during the first hydrogenation [9,10]. The line broadening has been reported to depend on the element substituted for Ni. For example, substitution of Al for the Ni in $LaNi_{5-x}Al_x$ at $x > 0.2$ causes the pressure difference and anisotropic line broadening to disappear [5].

Few microscopic studies on $LaNi_5$-based alloys have been carried out using transmission electron microscopy (TEM); instead, most of the past research has been based on X-ray and neutron diffraction analysis. It has been reported that stacking faults are present in (0 0 0 l) planes in the activated $LaNi_5$ and that the hydride precipitates in the form of thin plates along $< 2\bar{1}\bar{1}0 >$ to grow into large grains [11,12]. Yamamoto et al. have reported the formation of numerous a-type dislocations in the $LaNi_5$-based alloys after the first cycle of hydrogen absorption and desorption [13]. Finding that the difference in absorption pressure between the first and second cycles was caused by the generation of cracks and a-type dislocations with a Burgers vector of $1/3 < 11\bar{2}0 >$. On the other hand, cycling properties are typically evaluated in terms of the difference in equilibrium pressure between hydrogen absorption and desorption in the isotherm [14].

In the present study, the microstructure of $LaNi_5$-based alloys before and after hydrogen absorption/desorption cycling was investigated in detail by TEM, in order to elucidate systematically the lattice defects introduced during hydrogenation and dehydrogenation. Another aim of this work was to examine the structure of the interface between the hydride and the metal-hydrogen solution matrix. While a few structural model of hydride formation

* Corresponding author at: International Institute for Carbon-Neutral Energy Research (I2CNER), Kyushu University, 744 Motooka, Nishi-ku, Fukuoka 819-0395, Japan. Tel.: +81 92 802 3235.
*E-mail address:* junko.matsuda@i2cner.kyushu-u.ac.jp (J. Matsuda).

0925-8388/$ – see front matter © 2011 Elsevier B.V. All rights reserved.
doi:10.1016/j.jallcom.2011.04.096

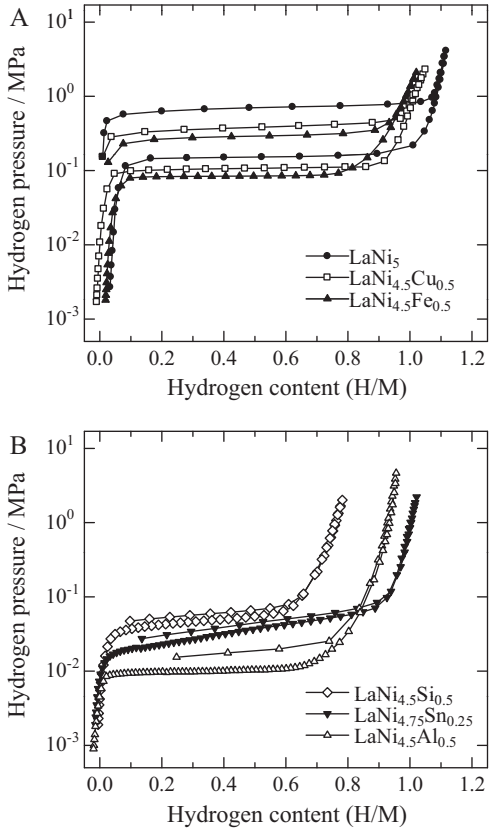


**Fig. 1.** *P–C* isotherms of first absorption/desorption cycle of $LaNi_5$, $LaNi_{4.5}M_{0.5}$ (M = Cu, Fe, Si, Al) and $LaNi_{4.75}Sn_{0.25}$ measured at 298 K under 5 MPa.

in pure Zr and V metals with equilibrium pressures greater than 0.1 MPa have been proposed [15,16], the present study was focused on $LaNi_5$-based alloys, which were selected as representative brittle intermetallic compounds. Because the hydrogen equilibrium pressure and cycling properties can be tuned by altering the constituent elements, this type of alloys is promising for practical applications such as Ni-MH batteries and stationary hydrogen storage.

## 2. Experimental

$LaNi_5$, $LaNi_{5-x}Fe_x$ ($x$ = 0.1–1.2) and $LaNi_{5-y}Al_y$ ($y$ = 0.05–0.5) were prepared by arc-melting and $LaNi_{4.5}Cu_{0.5}$, $LaNi_{4.5}Si_{0.5}$ and $LaNi_{4.75}Sn_{0.25}$ were prepared by high-frequency induction melting method. All specimens were annealed at 1173–1223 K for 48 h in evacuated silica tubes. Pressure–composition (*P–C*) isotherms were measured by the Sieverts method at 298 K after evacuation at 393 K. All annealed $LaNi_5$-based alloys were observed by TEM before hydrogenation, after the first cycle of hydrogen absorption/desorption and after the fifth cycle. Samples for TEM observation were prepared by two methods: (1) alloy particles before and after hydrogenation were dispersed on Cu mesh without carbon film, and (2) brass tubes filled with the alloy particles in epoxy resin were thinned by mechanically grinding, by dimpling and finally by ion milling using a liquid nitrogen cold stage. An H-9000NAR system, Hitachi High-Technologies Co., was used for TEM observation in this study.

## 3. Results and discussion

### 3.1. *P–C isotherms of* $LaNi_{5-x}M_x$

Fig. 1(a) and (b) shows the *P–C* isotherms of the first absorption/desorption cycle of $LaNi_5$, $LaNi_{4.5}M_{0.5}$ (M = Cu, Fe, Si, Al) and $LaNi_{4.75}Sn_{0.25}$. The difference in pressure between the first absorption and first desorption for $LaNi_{4.5}Cu_{0.5}$ and $LaNi_{4.5}Fe_{0.5}$ was similar to that for $LaNi_5$. On the other hand, $LaNi_{4.5}Si_{0.5}$, $LaNi_{4.5}Al_{0.5}$ and $LaNi_{4.75}Sn_{0.25}$ exhibited little or no hysteresis in the *P–C* isotherms: their first absorption and desorption equilibrium pressures were similar. The difference in equilibrium pressure between hydrogen absorption and desorption for $LaNi_5$, $LaNi_{4.5}Cu_{0.5}$ and $LaNi_{4.5}Fe_{0.5}$ tended to decrease as the cycle number increased. In addition, the hydrogen desorption pressures for all the $LaNi_5$-based alloys were constant after the first cycle.

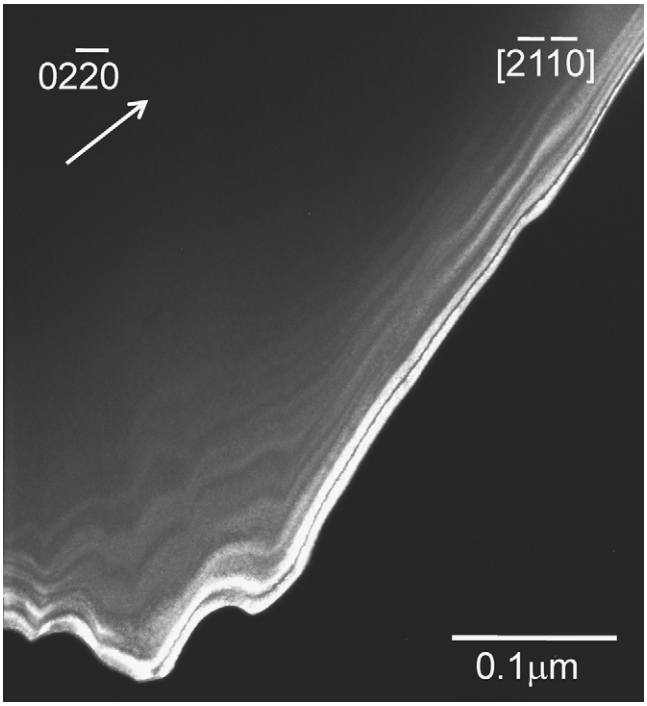


**Fig. 2.** Typical dark-field TEM image of $LaNi_{4.5}Fe_{0.5}$ before hydrogen absorption/desorption. Image was taken from [2 $\bar{1}$ $\bar{1}$ 0] with 0 2 $\bar{2}$ 0 reflection.

### 3.2. *Dislocation formation during hydrogen absorption and desorption cycling*

Fig. 2 shows a typical dark-field TEM image of $LaNi_{4.5}Fe_{0.5}$ before the first hydrogen absorption/desorption cycle. This image was taken from the [2 $\bar{1}$ $\bar{1}$ 0] direction with the 0 2 $\bar{2}$ 0 reflection. As shown in this image, bright-dark contrast due to lattice defects was not observed in this alloy before hydrogen absorption; fringe contrast is caused by the difference in sample thickness. Lattice defects such as dislocations and stacking faults were not found in any $LaNi_5$-based alloys before hydrogen absorption.

Fig. 3 shows TEM images of $LaNi_{4.5}Fe_{0.5}$ after the first hydrogen absorption–desorption cycle. In Fig. 3(a), bright lines corresponding to a-type dislocations along to the ($\bar{1}$ 2 $\bar{1}$ 0) plane can be seen for this sample. Fig. 3(b) shows that the c-type dislocations along to the (0 0 0 1) plane were also formed after the first hydrogen absorption/desorption cycle. These a-type and c-type dislocations were introduced with spacings of 10–20 nm and 100–200 nm, respectively, in both $LaNi_5$ and $LaNi_{4.5}Fe_{0.5}$. Dislocation density was estimated to be greater than or equal to $10^{11}$ $cm^{-2}$ from these spacings in $LaNi_5$ and $LaNi_{4.5}Fe_{0.5}$. After the first absorption/desorption cycle, $LaNi_{4.5}Cu_{0.5}$ exhibited a-type and c-type dislocations with spacings of 20–50 nm and 200–500 nm, respectively. In this case, the dislocation densities were $10^{11}$ and $10^{10}$ $cm^{-2}$, respectively.

Fig. 4(a) and (b) shows TEM dark-field images of $LaNi_{4.75}Sn_{0.25}$ after one cycle and five cycles of hydrogen absorption–desorption, respectively. No dislocations or stacking faults were observed in $LaNi_{4.75}Sn_{0.25}$ after one cycle. However, a-type dislocations were formed in some particles after five cycles. This indicates that the number of dislocations increases as the cycle number increases,

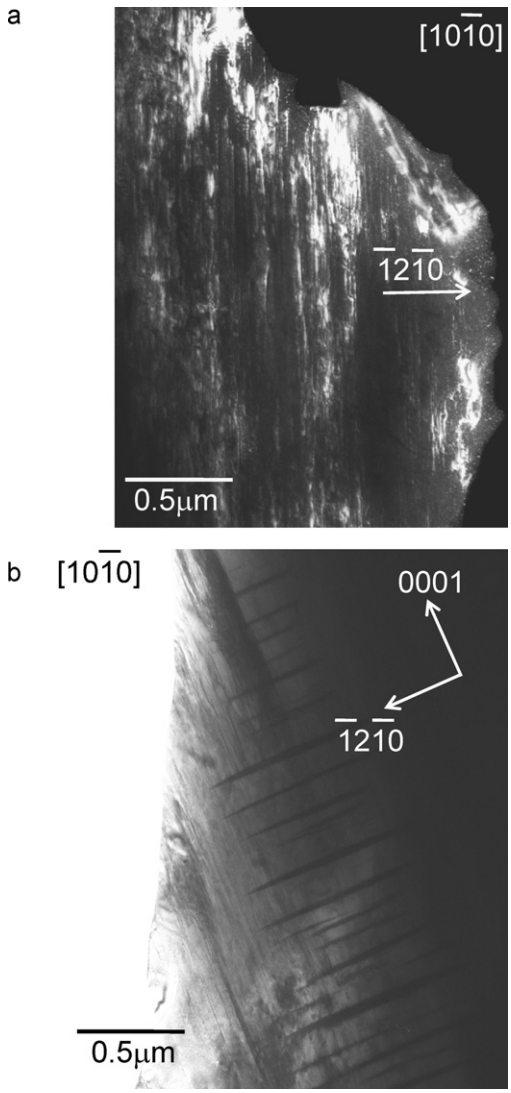


**Fig. 3.** TEM images of $LaNi_{4.5}Fe_{0.5}$ after the first cycle of hydrogen absorption/desorption: (a) the dark-field image taken from the direction of [1 0 $\bar{1}$ 0] with [$\bar{1}$ 2 $\bar{1}$ 0] reflection and (b) the bright-field image from [1 0 $\bar{1}$ 0] with 0 0 0 1 reflection.

although this trends depend on the particle size before hydrogenation; generally, larger particles are easily broken by stress concentration and smaller particles tend to undergo plastic deformation. As for $LaNi_{4.5}Si_{0.5}$ and $LaNi_{4.5}Al_{0.5}$, no dislocations were observed after five cycles of *P*–*C* measurements.

As described above, numerous a-type and c-type dislocations were introduced into $LaNi_5$, $LaNi_{4.5}Fe_{0.5}$ and $LaNi_{4.5}Cu_{0.5}$ after the first hydrogen absorption/desorption cycle. In the first cycle, these samples exhibited large differences between the absorption pressure and the desorption pressure. In contrast, no dislocations were formed in $LaNi_{4.5}Si_{0.5}$, $LaNi_{4.5}Al_{0.5}$ and $LaNi_{4.75}Sn_{0.25}$ after the first cycle. Table 1 lists the differences in equilibrium pressure between the first absorption and first desorption, as well as the dislocation densities after the first cycle of *P*–*C* measurements. A higher density of a-type dislocations than c-type dislocations corresponds to hk0 peak broadening in the XRD pattern of the $LaNi_5$ after hydrogen absorption/desorption. Yamamoto et al. have reported that almost all a-type dislocations were introduced during the first absorption/desorption cycle, whereas the dislocation density in TiFe alloys increased as the cycle number increased [17]. In the present study, the dislocation density in the $LaNi_5$-based alloys was also found to increase as the cycle number increased. These results suggest that

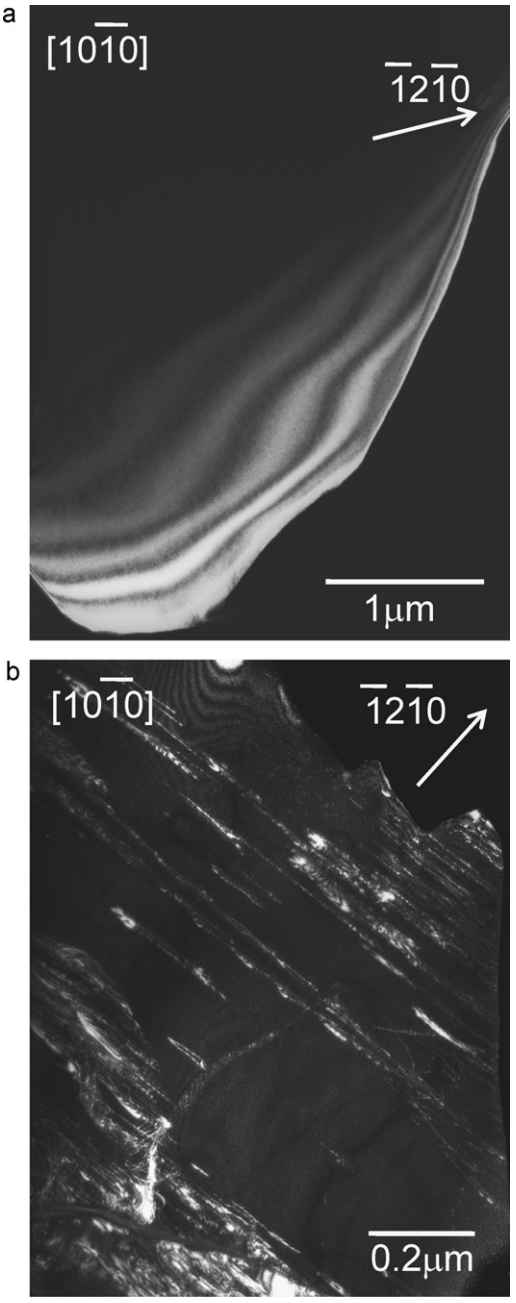


**Fig. 4.** Dark-field micrographs of $LaNi_{4.75}Sn_{0.25}$ (a) after one cycle and (b) after five cycles of hydrogen absorption and desorption, taken from the direction of [1 0 $\bar{1}$ 0] with $\bar{1}$ 2 $\bar{1}$ 0 reflection.

**Table 1**
Difference between the first absorption and desorption equilibrium pressures, and dislocation densities after the first cycle of *P*–*C* measurements.

| | $P_{a1} - P_{d1}$/MPa | a-Type dislocation | c-Type dislocation |
|---|---|---|---|
| $LaNi_5$ | 0.5219 | $>10^{11}$ cm$^{-2}$ | $10^{11}$ cm$^{-2}$ |
| $LaNi_{4.5}Fe_{0.5}$ | 0.2112 | $>10^{11}$ cm$^{-2}$ | $10^{11}$ cm$^{-2}$ |
| $LaNi_{4.25}Fe_{0.75}$ | 0.1457 | $>10^{11}$ cm$^{-2}$ | $10^{10}$ cm$^{-2}$ |
| $LaNi_4Fe$ | 0.0805 | $10^{11}$ cm$^{-2}$ | $10^{10}$ cm$^{-2}$ |
| $LaNi_{4.5}Cu_{0.5}$ | 0.2742 | $10^{11}$ cm$^{-2}$ | $10^{10}$ cm$^{-2}$ |
| $LaNi_{4.5}Si_{0.5}$ | 0.0091 | – | – |
| $LaNi_{4.75}Sn_{0.25}$ | 0.0072 | ($<10^{11}$ cm$^{-2}$)[a] | – |
| $LaNi_{4.95}Al_{0.05}$ | 0.3432 | $>10^{11}$ cm$^{-2}$ | $10^{11}$ cm$^{-2}$ |
| $LaNi_{4.9}Al_{0.1}$ | 0.2662 | $>10^{11}$ cm$^{-2}$ | $10^{10}$ cm$^{-2}$ |
| $LaNi_{4.75}Al_{0.25}$ | 0.0393 | $10^{11}$ cm$^{-2}$ | – |
| $LaNi_{4.5}Al_{0.5}$ | 0.0084 | – | – |

[a] After five cycles of hydrogen absorption/desorption.

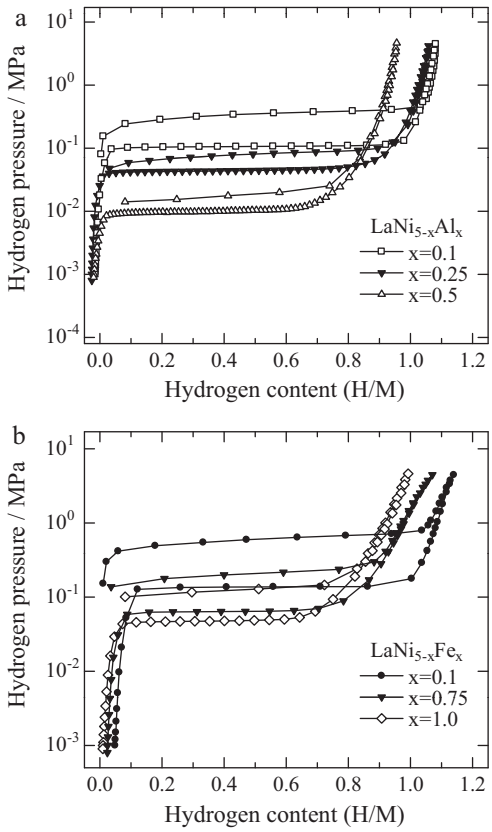


**Fig. 5.** *P–C* isotherms of first absorption/desorption cycle for (a) $LaNi_{5-x}Al_x$ ($x$ = 0.1, 0.25, 0.5) and (b) $LaNi_{5-x}Fe_x$ ($x$ = 0.1, 0.75, 1.0), measured at 298 K under 5 MPa.

excess pressure is needed in the hydrogen absorption process for the formation of misfit dislocations in the $LaNi_5$-based alloys.

### 3.3. Relationship between the amount of substitution and dislocation density in $LaNi_5$-based alloy

It has been reported that Al can be substituted for Ni in $LaNi_{5-x}Al_x$ up to $x$ = 1.3, and Fe can be substituted for Ni in $LaNi_{5-y}Fe_y$ up to $y$ = 1.2. Nickel is replaced by Fe at both the 2c and 3g sites, whereas substitution with Al occurs at only the 3g site [3,16]. Fig. 5 shows *P–C* isotherms of $LaNi_{5-x}M_x$ (M = Al, Fe). As shown in Fig. 5(a), the difference between the first absorption and desorption pressures decreased to less than 0.1 MPa in $LaNi_{5-x}Al_x$ if $x$ was larger than 0.2. In contrast, in Fe-substituted $LaNi_5$, the hysteresis in the *P–C* isotherms was not reduced as the amount of Fe was increased, although the first equilibrium absorption pressure and the maximum hydrogen content decreased with increasing Fe substitution. In order to investigate the effect of the amount of substitution on the microstructural evolution during the reaction, we observed $LaNi_{5-x}Al_x$ and $LaNi_{5-y}Fe_y$ before and after hydrogen absorption/desorption cycles by TEM.

Both a-type and c-type dislocations were introduced in all of the $LaNi_{5-x}Fe_x$ ($x$ = 0.05–1.2) specimens after the first cycle of hydrogen absorption and desorption, and dislocation density decreased as the difference in equilibrium pressure between the first absorption and first desorption decreased when $x$ was larger than 0.5. In $LaNi_4Fe$ and $LaNi_{3.8}Fe_{1.2}$, the differences in equilibrium pressure between the first absorption and first desorption were less than 0.1 MPa, 0.0805 MPa and 0.0465 MPa, respectively. In these samples, the density of c-type dislocations was $10^{10}$ $cm^{-1}$.

Fig. 6 shows that when $x$ was not greater than 0.1, a-type and c-type dislocations were introduced into $LaNi_{5-x}Al_x$ ($x$ = 0.05–0.5) after the first cycle of hydrogen absorption/desorption. In $LaNi_{4.75}Al_{0.25}$, some particles exhibited a-type dislocations after the first cycle. However, no lattice defects such as a-type and c-type dislocations were observed and only microcracks were observed in the $LaNi_{4.5}Al_{0.5}$ particles.

### 3.4. Formation mechanism of dislocations during hydrogenation

Hysteresis in *P–C* isotherms of metal hydrides such as the Pd–H system has been extensively researched in the past 50 years. The hysteresis is generally attributed to the increase in the free energy of the hydride phase due to mechanical strain in the lattice and to the effect of nucleus size. In apparent equilibrium, it is argued that more than one pressure was possible for the same concentrations of hydrogen [18,19]. Schultus and Hall note that hysteresis resulted from plastic deformation during the formation of the hydride phase in the Pd–H system [20]. They assumed that strain was absent or greatly reduced during dehydrogenation, and represented the hysteresis gap pressure ratio as $(p_f/p_d)^{1/2} = \exp(V_H \Delta p/RT)$, where $p_f$ and $p_d$ refer to the formation and deformation pressures of hydrogen, $V_H$ is partial molar volume of hydrogen and $\Delta p$ is approximately equal to the elastic limit of palladium. Flanagan and Clewley explained that the energy required to form new dislocations subsequently appeared as heat that transferred to the surroundings, resulting in increased chemical potential of metal phases both during hydride formation and deformation [14].

In the present work, we have focused on the difference between hydrogen absorption and desorption pressures, and we propose that the formation of dislocations leads to the difference in equilibrium pressure between hydrogen absorption and desorption. As described in Section 3.1, the hydrogen desorption pressure was independent of cycle number in all of the $LaNi_5$-based alloys investigated in the present work. However, the difference in pressure between the first absorption and first desorption strongly depended on the degree of substitution of a third element into $LaNi_5$. On the basis of in situ XRD results, dislocations can be considered to be introduced during the hydrogen absorption process [9]. With those results borne in mind, we discuss the relationship between hydrogenation and the formation of a-type and c-type dislocations, taking into account the difference between the absorption and desorption pressures required for introducing dislocations in $LaNi_5$-based alloys during hydrogenation.

The a-type and c-type dislocations are edge dislocations with the Burgers vectors of $1/3 < \bar{2}\,1\,1\,0 >$ and <0 0 0 1>, respectively, on the $\{0\,1\,\bar{1}\,0\}$ slip plane in the hexagonal crystal. These a-type and c-type dislocations are considered to be misfit dislocations that accommodate the lattice mismatch between the metal-hydrogen solid solution and the hydride. From the results reported here we can infer that the interface between the solid solution and hydride is possibly on the $\{0\,1\,\bar{1}\,0\}$ planes. Fig. 7 shows a schematic diagram of the structure of the interface between the solution and hydride during hydrogen absorption. In this case, compressive stress and tensile stress, respectively, increase in the solid solution and hydride along the interface. When the thickness of the hydride reaches a critical thickness, misfit dislocations are formed in the hydride, which has a smaller elastic constant than the metal-hydrogen solid solution. The elastic constants were estimated by first-principles calculations [21,22] and the spacing of misfit dislocations ($\Delta$) was calculated as follows:

$$\Delta = \frac{a_\alpha a_\beta}{a_\alpha - a_\beta}$$

where $a_\alpha$ and $a_\beta$ are the lattice parameters of solid solution ($\alpha$) and hydride ($\beta$).

From this equation, the spacings of a-type and c-type dislocations in $LaNi_{4.8}Fe_{0.2}$ were calculated to be 8 nm and 7.1 nm,

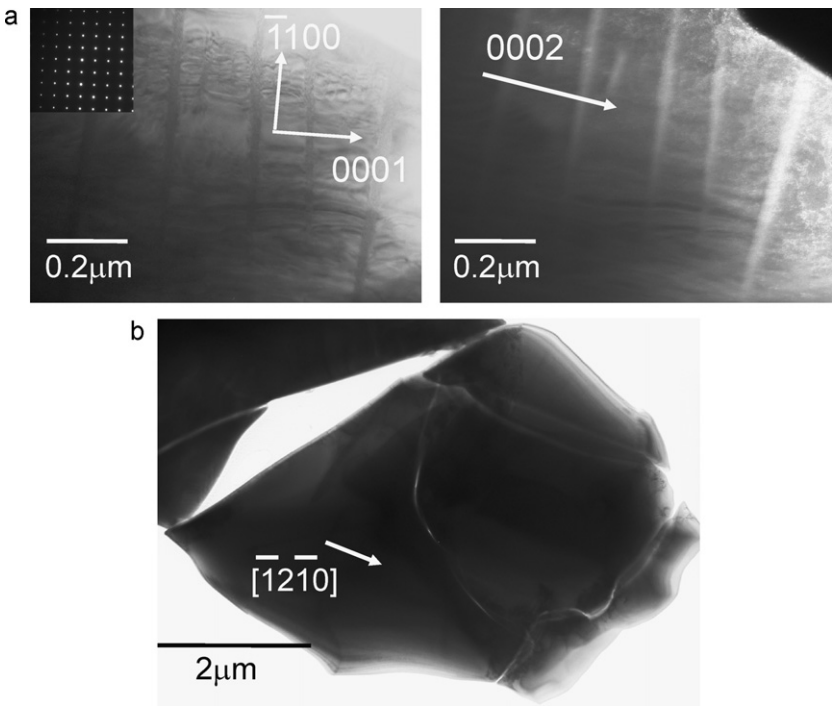


**Fig. 6.** (a) Bright-field image of $LaNi_{4.9}Al_{0.1}$ after first cycle, which was observed from [1 1 $\bar{2}$ 0], (b) dark-field image of $LaNi_{4.9}Al_{0.1}$ taken from [1 1 $\bar{2}$ 0] with 0 0 0 2 reflection, and (c) bright-field image of $LaNi_{4.5}Al_{0.5}$ after the fifth cycle, which were taken from [$\bar{1}$ 0 $\bar{1}$ 0] with $\bar{1}$ 2 $\bar{1}$ 0 reflection. Images in (a) and (b) were taken from the same position.

respectively. In addition, the spacings of a-type and c-type dislocations in $LaNi_{4.75}Sn_{0.25}$ were calculated to be 11.0 nm and 16.6 nm, respectively. These calculated spacings are of the same order as those observed for a-type dislocations in the $LaNi_5$, $LaNi_{4.5}Cu_{0.5}$ and $LaNi_{4.5}Fe_{0.5}$ which exhibited the large difference in pressure between hydrogen absorption and desorption. However, the observed dislocation spacings in $LaNi_{4.5}Si_{0.5}$, $LaNi_{4.5}Al_{0.5}$ and $LaNi_{4.75}Sn_{0.25}$ which showed little or no hysteresis did not agree with the calculated values. Moreover, the observed spacing of c-type dislocations in all the $LaNi_5$-based alloys studied did not agree with the predicted values. Possible reasons for this disagreement include (1) a preferred growth direction and orientation relationship of the hydride relative to the solid solution matrix, depending on the element substituted into the $LaNi_5$-based alloys; and (2) volume expansion during hydrogenation resulting in generation of cracks before the introducing of dislocations, because the plasticity of the $LaNi_5$-based alloys is also affected by the substituted elements. In fact, during the first hydrogenation the particle size of the $LaNi_5$–H decreased to about 100 μm from 100 to 1000 μm: in contrast, the particle size of $LaNi_{4.5}Al_{0.5}$–H was found to decrease to less than 50 μm in this study. This result indicates that Al-substituted $LaNi_5$ alloys do not require excess absorption pressure for the introducing of dislocations because the formation of cracks occurs readily during hydrogenation.

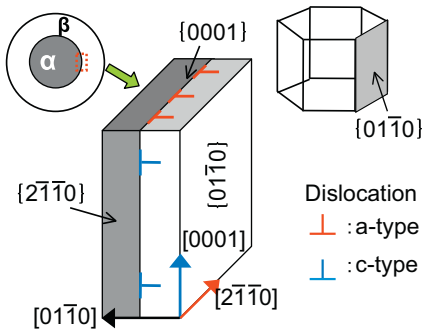


**Fig. 7.** Schematic diagram of interfacial structure between metal-hydrogen solid solution and metal hydride during hydrogen absorption for the $LaNi_5$-based alloy system.

## 4. Conclusions

The microstructural evolution of $LaNi_5$-based alloys before and after hydrogen absorption/desorption cycles has been investigated by transmission electron microscopy. It was found that dense a-type and c-type dislocations were introduced into $LaNi_5$, $LaNi_{4.5}Cu_{0.5}$ and $LaNi_{4.5}Fe_{0.5}$ after the first hydrogen absorption/desorption cycle. These alloys exhibited large differences in the equilibrium hydrogen pressures of hydrogenation and dehydrogenation. Both a-type and c-type dislocations have Burgers vectors of $1/3 < 1\,1\,\bar{2}\,0 >$ and <0 0 0 1>, respectively, on the {0 1 $\bar{1}$ 0} slip plane. These dislocations were introduced in order to accommodate lattice mismatch between the hydrogen-metal solid solutions and metal hydrides. The interface between the solid solution and hydride was suggested to be the {0 1 $\bar{1}$ 0} planes. In contrast, dislocations and stacking faults were not observed in $LaNi_{4.5}Si_{0.5}$, $LaNi_{4.5}Al_{0.5}$ and $LaNi_{4.75}Sn_{0.75}$, which exhibited little or no difference in the equilibrium pressure between the first absorption and first desorption. From these experimental results, we conclude that the difference between the absorption and desorption pressures is due to the generation of misfit dislocations. $LaNi_5$-based alloys, in which mechanical strain was accommodated by the generation of cracks before the introducing of dislocations, exhibited small hysteresis in *P–C* isotherms.

## Acknowledgment

This work was supported by The New Energy and Industrial Technology Development Organization (NEDO) under Advanced Research on Hydrogen Storage Materials (HYDRO-STAR).

## References


[1] J.H.N. Van Vucht, F.A. Kuijpers, H.C.A.M. Bruning, Philips Res. Repts. 25 (1970) 133.
[2] H.H. Van mal, K.H.J. Buschow, A.R. Miedema, J. Less-Common Met. 35 (1974) 65–76.
[3] A. Percheron-guegan, C. Lartigue, J.C. Achard, J. Less-Common Met. 109 (1985) 287–309.
[4] J.J. Reilly, G.D. Adzic, J.R. Johnson, T. Vogt, S. Mukerjee, J. McBreen, J. Alloys Compd. 293–295 (1999) 569–582.
[5] A. Percheron-Guegan, C. Lartigue, P. Germi, F. Tasset, J.C. Achard, J. Less-Common Met. 74 (1980) 1–12.
[6] M.H. Mendelsohn, D.H. Gruen, Mater. Res. Bull. 13 (1978) 1221–1224.
[7] E. Akiba, H. Hayakawa, Y. Ishido, K. Nomura, S. Shin, T. Minesawa, MRS Intl. Mtg. Adv. Mats. 2 (1989) 39–44.
[8] T. Sakai, K. Oguro, H. Miyamura, N. Kuriyama, A. Kato, H. Ishikawa, C. Iwakura, J. Less-Common Met. 161 (1990) 193–202.
[9] Y. Nakamura, E. Akiba, J. Alloys Compd. 298 (2000) 138–145.
[10] Y. Nakamura, R.C. Bowman, E. Akiba, J. Alloys Compd. 373 (2004) 183–193.
[11] E.H. Kisi, C.E. Buckley, E.M. Gray, J. Alloys Compd. 185 (1992) 369–384.
[12] G.-H. Kim, C.-H. Chun, S.-G. Lee, J.-Y. Lee, Acta Metall. Mater. 42 (1994) 3157–3161.
[13] T. Yamamoto, H. Inui, M. Yamaguchi, Intermetallics 9 (2001) 987–991.
[14] T.B. Flanagan, J.D. Clewley, J. Less-Common Met. 83 (1982) 127–141.
[15] M.P. Cassidy, B.C. Muddle, T.E. Scott, C.M. Wayman, J.S. Bowles, Acta Metall. 25 (1977) 829–838.
[16] G.J.C. Carpenter, Acta Metall. 26 (1978) 1225–1235.
[17] H. Inui, T. Yamamoto, M. Hirota, M. Yamaguchi, J. Alloys Compd. 330–332 (2002) 117–124.
[18] A.R. Ubbelohde, Proc. R. Soc. London A 159 (1937) 295.
[19] J.R. Lacher, Proc. R. Soc. London A 161 (1937) 525.
[20] N.A. Schultus, W.K. Hall, J. Chem. Phys. 39 (1963) 868.
[21] K. Tatsumi, I. Tanaka, K. Tanaka, H. Inui, M. Yamaguchi, H. Adachi, M. Mizuno, J. Phys. Condens. Matter 15 (2003) 6549–6561.
[22] L.G. Hector Jr., J.F. Herbst, T.W. Capehart, J. Alloys Compd. 353 (2003) 74–85.